Risk Stratification of Colon Carcinogenesis through Enhanced Backscattering Spectroscopy Analysis of the Uninvolved Colonic Mucosa

Hemant K. Roy,[1] Young L. Kim,[2] Yang Liu,[2] Ramesh K. Wali,[1] Michael J. Goldberg,[1] Vladimir Turzhitsky,[2] Jonathan Horwitz,[1] and Vadim Backman[1,2]

Abstract

Introduction: Our group has been interested in applying advances in biomedical optics to colorectal cancer risk stratification. Through a recent technological breakthrough, we have been able to harness information from enhanced backscattering spectroscopy, an optics phenomenon that allows quantitative, depth-selective analysis of the epithelial microscale/nanoscale architecture. In the present study, we investigated the ability of enhanced backscattering analysis of the preneoplastic mucosa to predict risk of colon carcinogenesis.

Methods: Enhanced backscattering analysis was done on intestinal mucosa at preneoplastic time points from two experimental models of colorectal cancer: the azoxymethane-treated rat and the multiple intestinal neoplasia (MIN) mouse. Data were analyzed using two previously validated spectral markers: spectral slope and principle components. We then did a pilot study on mucosal biopsies from 63 subjects undergoing screening colonoscopy.

Results: In the azoxymethane-treated rat, when compared with saline-treated controls, significant changes in the enhanced backscattering markers were observed as early as 2 weeks after azoxymethane treatment (before the development of aberrant crypt foci and adenomas). Enhanced backscattering markers continued to progress over time in a manner consonant with future neoplasia. These data were replicated in the preneoplastic MIN mouse mucosa. In humans, spectral slopes in the endoscopically normal cecum, midtransverse colon, and rectum were markedly reduced in patients harboring adenomas when compared with those who were neoplasia free.

Conclusions: We show, for the first time, that enhanced backscattering analysis of an aliquot of uninvolved mucosa has the potential for predicting neoplastic risk throughout the colon in both experimental colorectal cancer models and humans.

Colorectal cancer remains the second leading cause of cancer mortality in the United States. Although the survival for early-stage colorectal cancer is excellent, given the insidious nature of colonic neoplasia, most patients present at a more advanced stage (1). This underscores the necessity for comprehensive screening of the asymptomatic population. Direct visualization of the colon through endoscopy (flexible sigmoidoscopy or colonoscopy) has been shown to be effective in reducing colorectal cancer mortality as well as incidence (through identification and removal of the precursor lesion, the adenomatous polyp; ref. 2). However, the majority of the population does not undergo any endoscopic screening largely due to reluctance of both patients and physicians (3). Therefore, interest has focused on applying biomedical advances to devise more acceptable, cost-effective colorectal cancer screening approaches. Numerous techniques have been introduced with much fanfare but, to date, have failed to show the robustness necessary for population screening. For instance, the first reports of outstanding performance characteristics of fecal DNA analysis (4) were not born out in multicenter trials (5). From a radiological perspective, in initial single center studies, computed tomography colography (virtual colonoscopy) showed great promise (6); unfortunately, its sensitivity in multicenter trials has been disappointing (7).

Therefore, it seems that colonoscopy will remain the "gold standard" for the foreseeable future. However, resource constraints and potential complications make it impractical to perform colonoscopy on the entire at-risk population (generally considered age, ≥50). Thus, identifying patients who are most likely to benefit from colonoscopy is of paramount importance. Many risk stratification techniques exploit the

Authors' Affiliations: [1]Department of Medicine, Evanston Northwestern Healthcare and [2]Biomedical Engineering Department, Northwestern University, Evanston, Illinois

Received 7/26/05; revised 10/12/05; accepted 10/24/05.

Grant support: NIH grants U01CA11125 and R01 CA112315, National Science Foundation grant BES-0238903, and The Wallace H. Coulter Foundation.

The costs of publication of this article were defrayed in part by the payment of page charges. This article must therefore be hereby marked *advertisement* in accordance with 18 U.S.C. Section 1734 solely to indicate this fact.

Note: Presented in part in abstract form at the 106th Digestive Disease Week Meetings, May 15-19, 2005 in Chicago, Illinois.

Requests for reprints: Hemant K. Roy, Feinberg School of Medicine at Northwestern University, Evanston Northwestern Healthcare Research Institute, 1001 University Place, Evanston, IL 60201. Phone: 847-570-2239; Fax: 847-733-5041; E-mail: h-roy@northwestern.edu.

doi:10.1158/1078-0432.CCR-05-1605

"field effect," the concept that assessment of biomarkers in one area of the colon should be able to determine the likelihood of current/future neoplastic lesions throughout the colon (8, 9). A commonly used clinical example is the identification of the distal adenoma on flexible sigmoidoscopy to predict the occurrence of neoplasia in the proximal colon (10). Other attempts include correlation of rectal aberrant crypt foci (ACF) using chromoendoscopy with colonic adenomas and carcinomas (11). Unfortunately, the performance characteristics of the existing markers remain suboptimal (e.g., the sensitivity and positive predictive value for the ability of flexible sigmoidoscopy to detect advanced proximal lesions are 40% and 6%, respectively; refs. 12, 13).

Thus, it is clear that currently available morphologic markers for the field effect are inadequate for risk stratification. Several lines of evidence suggest that the field effect has the potential of being exquisitely sensitive at identifying patients with colonic neoplasia. Numerous studies have reported that in the histologically normal mucosa of subjects harboring colonic neoplasia, there are profound genetic and epigenetic alterations in the field effect (14, 15). However, detecting these molecular events with a methodology that would be feasible in clinical practice has been challenging.

Biomedical optics represents a powerful means of probing epithelial cellular architecture and has clear applications for colorectal cancer screening given ready access of the distal colonic mucosa via either stand-alone fiber optical probes or endoscope-coupled devises. Our group, in collaboration with others, has pioneered the use of light scattering spectroscopy to detect dysplastic cells *in vivo* through analysis of nuclear size and chromatin content (16, 17). Furthermore, we have shown that light scattering spectroscopy can identify adenomatous change in the colon (18). However, light scattering spectroscopy is unable to detect the more subtle microarchitectural consequences of the molecular changes in the colonic field. Enhanced backscattering is an optical phenomenon that can provide quantitative information about the nanoscale composition of the epithelium. Enhanced backscattering, otherwise known as coherent backscattering, is a spectacular manifestation of the self-interference of light propagating in a random medium, such as biological tissue, which leads to an enhanced scattering peak in the backward direction (i.e., direction opposite to that of the light beam incident on tissue surface). Although the potential of enhanced backscattering is well established, application of this approach to tissue diagnosis has been stymied by numerous technical problems. These include the extremely narrow widths of the enhanced backscattering peaks in tissue (full width at half maximum ~0.001 degree) and excessive speckle. Indeed, to date, use of enhanced backscattering to interrogate tissue microarchitecture has been technically impossible.

We have recently overcome these hurdles by recording enhanced backscattering under low coherence illumination, which gives rise to >100 times broadened and speckle-free enhanced backscattering peaks (19–21). Moreover, we have shown that this low-coherence enhanced backscattering (LEBS) spectroscopy allows the analysis of tissue nanoarchitecture and microarchitecture. Additionally, LEBS enables accurate depth resolution from a few microns to several hundreds of microns below tissue surface through the analysis of the angular profile of an LEBS peak (which contains information about a wide range of tissue depths simultaneously). This novel feature of LEBS has not been achievable with conventional optical spectroscopy. Depth selectivity has important advantages in analyzing the colonic field effect given the biological heterogeneity of colonocytes in the crypt with the earliest changes in neoplasia occurring towards the base of the crypt (i.e., stem cell compartment; ref. 22). Moreover, depth selectivity of LEBS is required to address one of the most notorious problems in tissue spectroscopy: light absorption by submucosal hemoglobin can obscure endogenous spectral signatures of epithelial cells (23). LEBS spectroscopy solves this problem by enabling selective probing of the most superficial layer of tissue, which maximizes the probability of targeting the epithelium and minimizes the interference from photons penetrating into the submucosa. In the present study, we showed the use of enhanced backscattering to predict neoplastic risk at the earliest points of colon carcinogenesis using the azoxymethane-treated rat model. Furthermore, we duplicated these data in the multiple intestinal neoplasia (MIN) mouse. Finally, we showed the applicability of these results to humans with a pilot clinical trial.

Materials and Methods

Instrumentation. To overcome the limitations of conventional enhanced backscattering for tissue characterization, we developed a novel spectroscopic technique (LEBS spectroscopy) by combining enhanced backscattering measurements with low spatially coherent, broadband illumination and spectrally resolved detection (19–21). Figure 1 shows a schematic of our LEBS instrument. A beam of broadband cw-light from a 500-W xenon lamp (Spectra-Physics Oriel Instruments Corp., Stratford, CT) was collimated (divergence ~0.03-0.10 degree), polarized, and delivered onto a sample at 15-degree angle

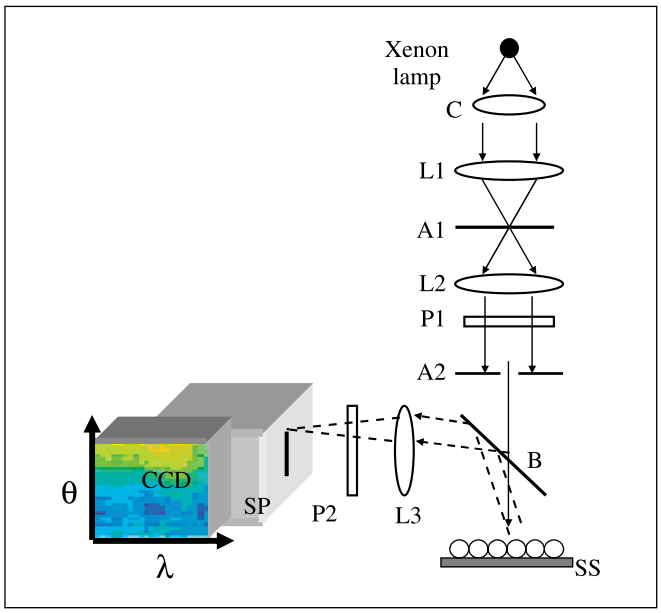

Fig. 1. LEBS spectroscopy instrument. C, condenser; L, lenses; A, apertures; P, polarizers; B, beam splitter; SS, sample stage; SP, spectrograph. The lens in the light collection arm of the instrument projects the angular distribution of backscattered light onto the slit of the imaging spectrometer. The spectrograph disperses scattered light in the direction perpendicular to the slit according to its wavelengths. Thus, the CCD records a matrix of enhanced backscattering intensity as a function of wavelength and scattering angle $I_{EBS}(\theta,\lambda)$.

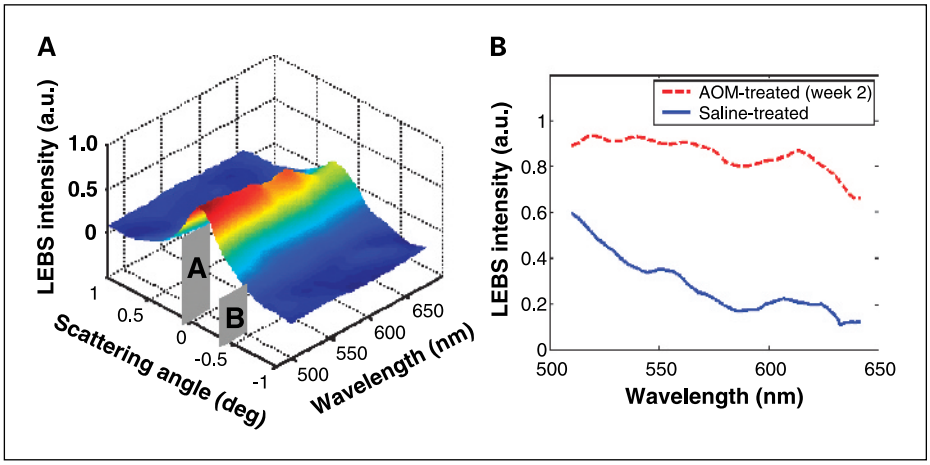

Fig. 2. *A*, representative LEBS intensity signal $I_{EBS}(\theta,\lambda)$ obtained from rat colonic tissue using the LCBS spectroscopy instrument. *B*, typical LEBS intensity spectra obtained from colonic tissues of azoxymethane (*AOM*) – treated rats (2 weeks after azoxymethane administration) and saline-treated rats. The LEBS spectra obtained from the azoxymethane-treated rats and the saline-treated rats are clearly different.

of incidence to prevent the collection of the specular reflection. The instrument allowed varying spatial coherence length L_{cs} of the incident light from 100 to 200 μm by means of aperture A1 positioned in the Fourier plane of lens system L1/L2 in the light delivery arm of the instrument. The spatial coherence length was confirmed by the double-slit interference (24). The light backscattered by a sample was collected using a Fourier lens L3, a polarizer P2 (oriented along the polarization of the incident light), and an imaging spectrograph SP (Acton Research, Acton, MA), which was positioned in the focal plane of the lens and coupled with a CCD camera (VersArray^{xp}, Roper Scientific, Trenton, NJ). The lens projected the angular distribution of the backscattered light onto the slit of the spectrograph. Thus, all scattered rays with an identical scattering angle θ were focused into a point on the entrance slit of the spectrometer. Then, the imaging spectrograph dispersed this light according to its wavelength in the direction perpendicular to the slit. Thus, the CCD recorded a matrix of light-scattering intensities as a function of wavelength λ and backscattering angle θ. In each CCD pixel, collected light was integrated within a certain narrow wavelength band $\Delta\lambda$ around λ. For each λ, the width of the band and, thus, temporal coherence length L_{ct} was determined by the width of the spectrograph slit. In the experiments reported below, L_{ct} was fixed at 30 μm ($\Delta\lambda$ = 9 nm).

Animal studies. All animal studies were approved and done in accordance with the institutional animal care and use committee of Evanston Northwestern Healthcare. Male Fisher 344 rats (100-150 g) were randomized to two weekly injection of azoxymethane (15 mg/kg i.p.; Sigma, St. Louis, MO) or saline. Animals were euthanized at specified time points (2, 4, or 6 weeks after carcinogen injection). Colons were removed, opened longitudinally, and washed. Enhanced backscattering analysis was done on fresh, unfixed colons within 1 hour of removal. Similarly, male MIN and control C57BL6 mice [wild type at the adenomatous polyposis coli (*APC*) locus; The Jackson Laboratory, Bar Harbor, ME] were sacrificed at 6 to 7 weeks of age. The intestinal mucosa underwent enhanced backscattering analysis as described above. In each LEBS measurement, light scattering data from a tissue area ~1 mm^2 were recorded. For each animal, LEBS data were recorded from at least 20 different tissue sites spaced uniformly across the surface of the colon (in case of azoxymethane/saline-treated rats) or small bowel (in case of MIN and control mice).

Human studies. The human studies were approved and done in accordance with the institutional review board at Evanston Northwestern Healthcare. After informed consent, 63 subjects scheduled for screening/surveillance colonoscopy at Evanston Hospital had six biopsies of endoscopically normal mucosa (two each from cecum, midtransverse colon, and rectum) at least 5 cm away from any neoplastic lesion. The exclusion criteria included colitis (either history of or on suspected on present colonoscopy), coagulopathy, or inability to give informed consent. LEBS analysis was done within 1 hour of tissue acquisition by observers blinded to clinical/endoscopic data. For each subject, LEBS data were recorded from ~16 tissue sites per each segment (i.e., cecum, midtransverse colon, and rectum).

Results

Enhanced backscattering signals can be detected from colonic tissue. As discussed above, to date, the observation of enhanced backscattering in tissue has been exceedingly difficult, and no attempts have been made to use enhanced backscattering for tissue diagnosis. On the other hand, LEBS recently developed by our group significantly simplifies the observation of enhanced backscattering in tissue. Consistent with our previous observations, we were able to detect a crisp enhanced backscattering peak from colonic tissue in both animals and humans (see below). For instance, Fig. 2A shows an LEBS signal $I_{EBS}(\theta,\lambda)$ collected from rat colonic tissue (L_{cs} = 140 μm). An enhanced backscattering peak can be clearly identified. Furthermore, this figure illustrates some of the major advantages of LEBS: LEBS peak is >100 times wider than conventional enhanced backscattering, which makes LEBS easy to observe; it is not obstructed by speckle and is recorded for a wide range of wavelengths (400-700 nm) simultaneously.

Figure 2B shows representative LEBS spectra recorded from rat colons of azoxymethane-treated rats at an early, pre-ACF stage of carcinogenesis (2 weeks after azoxymethane treatment), and age-matched control animal (saline treatment). These LEBS spectra $I_{EBS}(\lambda)$ were obtained from $I_{EBS}(\theta,\lambda)$ by integrating over backscattering angle θ. As shown in Fig. 2B, the LEBS spectra obtained from the preneoplastic and control colonic tissues are distinctly different. As discussed below, the quantitative analysis of such LEBS spectra revealed a number of highly significant spectral markers that were diagnostic for the earliest field changes in colon carcinogenesis.

Optimal depth for identifying field effect alterations in early colon carcinogenesis. As we have previously detailed (16–18), in LEBS, the depth resolution can be achieved by analyzing the angular profile of an enhanced backscattering peak that contains information about a wide range of tissue depths simultaneously (~30 to ~80 μm for the spatial coherence length used in our experiments). In brief, the periphery of the enhanced backscattering peak (i.e., large backscattering angles: angular region B in Fig. 2A) is primarily contributed by light that does

not penetrate deep into tissue and thus probes short tissue depths. On the other hand, the tip of the enhanced backscattering peak ($\theta \sim 0$ degree: region A in Fig. 2A) mainly depends on longer light paths, and the spectra evaluated for these small backscattering angles can be used to probe deeper tissue. We have established the dependence of the depth of penetration on the angle for which LEBS spectra are evaluated (18).

First, we identified the optimal depth of penetration for which LEBS markers are the most diagnostic. Because the scattering angles determine the depth of penetration we evaluated a series of angles that corresponded to 30, 50, and 75 μm depths (angles 0.4 degree, 0.2 degree, and 0 degree, respectively). We selected one pre-ACF time point in the azoxymethane-treated rat model (2 weeks after azoxymethane administration). LEBS signals $I_{EBS}(\theta,\lambda)$ were recorded from at least 20 tissue sites per animal equally distributed throughout colonic surface. LEBS spectra $I_{EBS}(\lambda)$ were calculated from these signals as previously discussed above for each tissue depth (19–21).

Spectral behavior of $I_{EBS}(\lambda)$ depends on the size distribution of light-scattering structures(8, 25). Generally, $I_{EBS}(\lambda)$ is a declining function of wavelength, and its steepness is related to the relative portion of structures of different sizes. Larger structures that approached micron and supramicron sizes (i.e., cellular organelles, etc.) tend to reduce the steepness of $I_{EBS}(\lambda)$, whereas smaller scatterers (sizes as small as ~20 nm) tend to increase the steepness of $I_{EBS}(\lambda)$ over wavelength. To characterize $I_{EBS}(\lambda)$ with a single variable, we obtained linear fits to $I_{EBS}(\lambda)$ using linear regression from 530 to 640 nm. The absolute value of the linear coefficient of the fit is referred to as the "LEBS spectral slope" and quantifies the dependence of an LEBS spectrum on wavelength. As shown in Fig. 3, signals recorded from ~75-μm depth gave the best distinction between the control and azoxymethane-treated rats. We did not look at deeper depths given that the signals recorded from deeper tissue are affected by hemoglobin absorption. In the following animal studies, we analyzed LEBS spectra obtained from this critical depth.

Temporal progression of LEBS markers of the field effect in the azoxymethane-treated rat. Because the carcinogenic effects of azoxymethane progress over time, we reasoned that for LEBS signals serving as an intermediate biomarker, we would expect the magnitude of alterations of LEBS markers to increase over time. As seen in Fig. 4A, LEBS spectral slope progressively decreased at these early stages (2, 4, or 6 weeks after carcinogen injection). In the azoxymethane-treated rats, the LEBS spectral slope was dramatically decreased as early as 2 weeks after the carcinogen treatment ($P < 0.00001$) and continued to decrease over the course of the experiment ($P < 0.0001$, ANOVA). Such a progressive and highly statistically significant alteration of the LEBS spectral slope serves as a strong argument for the neoplastic relevance of this LEBS marker.

However, spectral slope harnesses only a small proportion of LEBS information. To more fully appreciate the complexity of the information contained in LEBS spectra, we did principle component analysis. First, we determined which principal component was of interest. We found that in our tissue data, the first two principal components (PC1 and PC2) accounted for ~99% of the data variance. We searched diagnostic principle components as a linear combination of PC1 and PC2 and identified principle component marker = PC1 + 5PC2 to be the significant. Therefore, LEBS principle component marker can be used as a convenient means to characterize the light scattering data. Once again, we found that LEBS principle component marker was significantly decreased at the 2-week time point ($P < 0.02$) and continued to progressively decrease over the course of the experiment ($P < 0.000001$; Fig. 4B).

LEBS markers in the MIN mouse. Although the azoxymethane-treated rat model is robust and well validated, to ensure that the changes in LEBS signatures are not model specific, we confirmed the findings in an alternate model of intestinal carcinogenesis, the MIN mouse. This is a genetic model with a germ line mutation in the APC, the initiating mutation in most sporadic colon carcinogenesis. These animals spontaneous develop intestinal adenomas starting at ages 9 to 10 weeks (25). We compared the LEBS signatures obtained from the MIN mice with age-matched negative control C57Bl mice. The control C57Bl mice differ from the MIN mice only in that they harbor a wild-type *APC* gene. The study involved $n = 18$ animals (nine MIN and nine control mice). For each animal, LEBS data were recorded for at least 20 different tissue sites spaced uniformly across the surface of the small bowel. We found that the LEBS markers that were significant for early

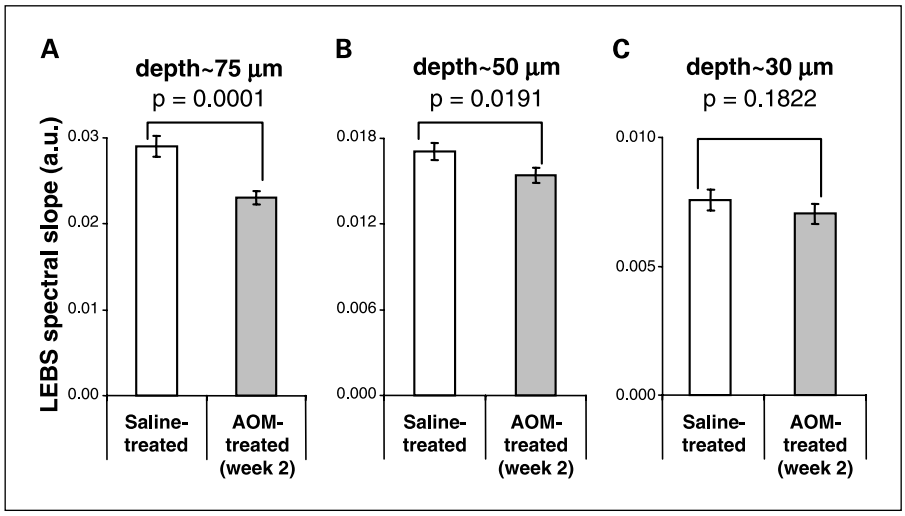

Fig. 3. LEBS spectral slopes obtained from rat colonic tissues 2 weeks after azoxymethane (*AOM*) administration compared with the saline-treated rats: (*A*) the lower compartment (~75 μm), (*B*) the middle compartment (~50 μm), and (*C*) the upper compartment (~30 μm) of the colonic mucosa. The optimal depth of penetration for the most diagnostic marker is identified as ~75-μm depths corresponding to the scattering angle of 0 degree.

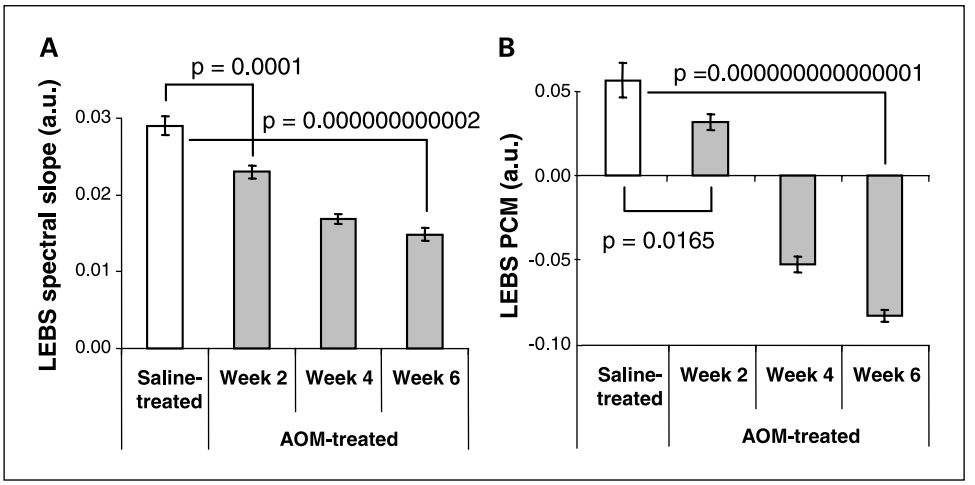

Fig. 4. *A,* changes in the LEBS spectral slope obtained from rat colonic tissue in 2, 4, and 6 weeks after azoxymethane (*AOM*) administration compared with the saline treated rats. *B,* changes in the LEBS principle component marker (*PCM*) obtained from rat colonic tissue in 2, 4, and 6 weeks after azoxymethane administration compared to the saline treated rats. The changes in both the LEBS spectral slope and the LEBS principle component marker follow the temporal progression of carcinogenesis.

colon carcinogenesis in the azoxymethane-treated rats were also diagnostic for the early preadenoma stage of intestinal neoplasia in the 6-week-old MIN mice. Specifically, we evaluated the intestinal mucosa at week 6 when the mucosa is histologically normal. As shown in Fig. 5, at this preneoplastic time point, there were dramatic alterations in both the LEBS spectral slope ($P < 0.01$) and LEBS principle component marker ($P < 0.01$). This highlights the robustness of our findings.

Pilot human data. To assess whether our findings in the azoxymethane-treated rat and MIN mouse could be translated into humans, we did a pilot human study in which we assessed LEBS spectral slope using *ex vivo* tissue from 63 subjects undergoing colonoscopy. The mean age of the subjects was 56.8 ± 10.7 years with 53% being female. We defined a low-risk group as those without personal history of neoplasia (both current and previous colonoscopies) and no family history of adenomas/carcinomas. Twenty patients were noted to have adenomas on current colonoscopy, and these lesions were relatively uniformly distributed between the right and left colon. All adenomas were histologically confirmed.

As discussed above, the LEBS data were obtained from endoscopically normal rectum, midtransverse colon, and the cecum at least 5 cm away from any neoplastic lesion. Figure 6 shows that there was a significant decrease in the spectral slope obtained from each of these three segments in patients who harbored adenomas somewhere in their colon when compared with those who were neoplasia free ($P < 0.01$). The magnitude of decrease of spectral slope seemed to be greater if the lesion was located in the same region as the LEBS analysis; however, significant differences were noted from LEBS measurements taken at distant sites (e.g., cecal LEBS spectral slope in patients with rectal adenomas). It needs to be emphasized that the post hoc analysis (effect of distance from neoplasm on spectral slope decrease) with relatively small numbers must be viewed with caution. We point out that the decrease of the spectral slope was consistent with a similar alteration of this marker in the azoxymethane-treated rat and MIN mouse models. These results support the hypothesis that alteration of light scattering; thus, nanoarchitectural/microarchitectural signatures in the uninvolved mucosa in humans (i.e., the field effect) is detectable by LEBS. Therefore, LEBS readings in easily accessible colonoscopically normal mucosa (e.g., in the rectum) have the potential to serve as accurate markers of the risk of neoplasia elsewhere in the colon.

Performance characteristics of LEBS markers. We calculated the sensitivity and specificity of LEBS markers for predicting neoplastic risk. As shown in Table 1, the performance characteristics of LEBS markers in the azoxymethane-treated rat were good at the pre-ACF phase (week 2) and perfect at a later stage (week 6), when ACF may occur but before adenoma development. Similar results were noted in the preneoplastic

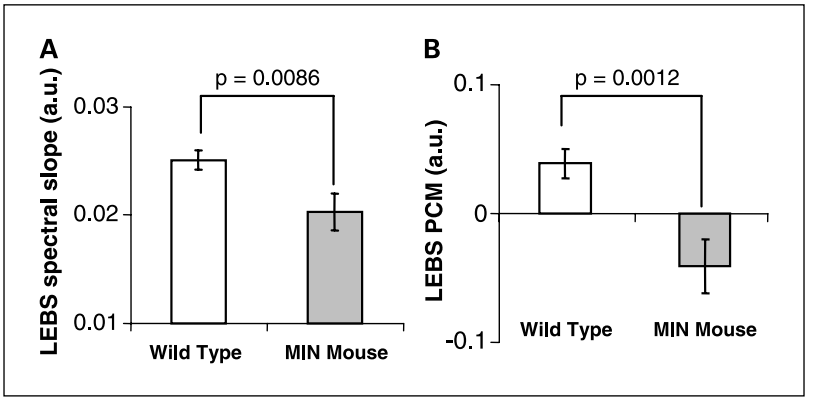

Fig. 5. LEBS spectral slope (*A*) and LEBS principle component marker (PCM; *B*) recorded from the uninvolved MIN mouse mucosa (distal small bowel) are significantly altered in the 6-week-old MIN mice when compared with age-matched mice that were wild-type for *APC* loci.

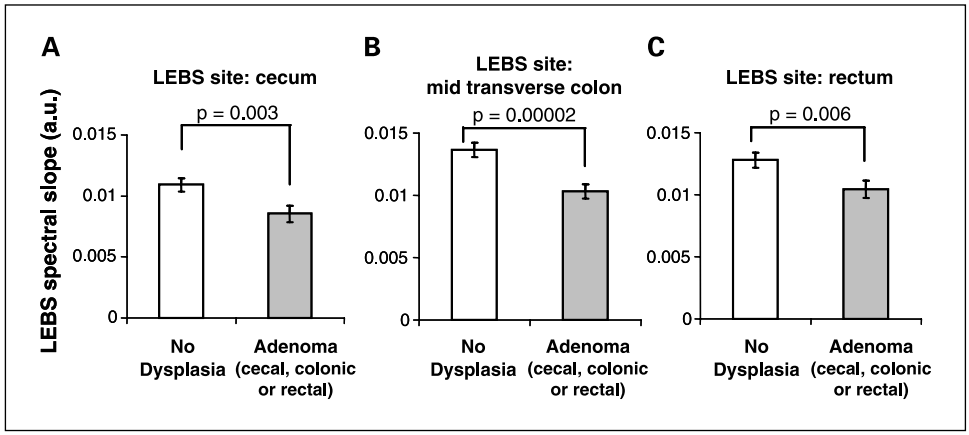

Fig. 6. Pilot human studies ($n = 63$ subjects). LEBS spectral slopes were assessed in (*A*) the cecum, (*B*) the midtransverse colon, and (*C*) the rectum of subjects undergoing colonoscopy. The subjects were divided into two groups as follows. High-risk group included subjects with adenomas anywhere in the colon. Low-risk group included patients with no personal or family history of colonic neoplasia. The LEBS spectral slope recorded from uninvolved mucosa was significantly lower in patients with adenomas compared with one recorded from the low-risk group subjects ($P < 0.01$).

MIN mouse mucosa. Finally, our clinical data suggest that rectal LEBS had excellent sensitivity and good specificity for the presence colonic of advanced adenomas (≥1 cm, villous features or high-grade dysplasia). Our findings suggest that the magnitude of alterations in LEBS markers (e.g., LEBS spectral slope) was greater in patients with more advanced lesions compared with simple adenomas (data not shown). However, we need to be circumspect regarding conclusions given the pilot nature of the clinical data.

Discussion

We show herein, for the first time, that a novel optics technology (LEBS) was able to identify colon carcinogenesis risk through detection of the field effect. Our data in the azoxymethane-treated rat model of colon carcinogenesis show alterations in LEBS markers at time points that precede ACF or adenoma formation (8). Furthermore, these markers progress over time consonant with the progression of carcinogenesis. These results were replicated in the genetic model of intestinal carcinogenesis (the MIN mouse), providing compelling evidence for the robustness of the findings. Finally, in pilot human studies, we observed that LEBS analysis of the endoscopically normal mucosa was able to detect differences in patients who harbored adenomas when compared with those who were neoplasia free. Thus, the technical advance of LEBS may potentially translate into a practical means for colon cancer screening.

As previously discussed, the exploitation of the field effect is a common strategy in colorectal cancer screening (e.g., assessment of distal adenomas or ACF). To improve sensitivity, others have proposed looking at cellular (apoptosis and proliferation; refs. 26, 27) and biochemical variables (e.g., protein kinase C; ref. 28); however, although somewhat of an improvement, the performance characteristics are still suboptimal for clinical practice. In the present study, our assessment of mucosal nanoarchitectural and microarchitectural markers by means of LEBS far outdid the classic morphologic or biochemical markers. Our approach was not to detect morphologic lesions (polyps) but rather to assess the risk of neoplasia from assessing the visually normal colonic mucosa. There is ample evidence to support the molecular underpinnings of the microarchitectural changes noted in the histologically normal "field." For instance, Chen et al. recently reported that a panel of proto-oncogenes, including cyclooxygenase 2 and osteopontin, were markedly overexpressed in histologically normal mucosa of patients harboring colorectal cancer (14). They also noted this in the preneoplastic MIN mouse and, importantly, the magnitude of proto-oncogenes overexpression was in-between control intestinal epithelium (C57BL/6 mice wild type at APC) and adenomatous tissue, arguing for the relevance of these changes to tumorigenesis (14). Furthermore, work by Cui et al. have noted that another epigenetic event (loss of insulin growth factor II imprinting) was increased in the uninvolved mucosa of patients with who harbored adenomas (15).

Our approach has been to evaluate nanoarchitectural/microarchitectural consequences of these genetic/epigenetic changes to risk stratify for colorectal cancer. Light scattering is determined by the fundamental properties of the scattering

Table 1. Sensitivity and specificity of LEBS markers for predicting neoplastic risk

	AOM-treated versus saline-treated rat (%)		MIN versus wild-type mice (%)	Patients with advanced adenomas versus neoplasia-free controls (%)
	2 wks after AOM treatment	6 wks after AOM treatment		
Sensitivity	84	100	88	100
Specificity	72	100	76	64

NOTE: The performance characteristics were calculated for AOM-treated rats (compared with age-matched, saline-treated controls) at pre-ACF (2 weeks) and preadenoma (6 weeks) time points. The MIN mice data were obtained at a preadenoma time point (week 6). The pilot human data were obtained from the endoscopically normal mucosa at least 5 cm from any neoplastic lesion and correlated with advanced adenoma occurrence elsewhere in the colon.

particles and thus represents a powerful, practical means of nanoarchitectural/microarchitectural assessment. Although there are a number of technological means for analyzing backscattered information, few have been able to quantitatively assess the nanoscale architecture. Enhanced backscattering is a unique multiple light-scattering phenomenon that encodes data regarding the characteristics of particles at the nanometer to micron scales. In contrast to the other light scattering–based techniques, enhanced backscattering originates from constructive interference of waves traveling in time-reversed paths (i.e., the paths whose first and last points coincide with the last and first points of its time-reversed counterpart, respectively). If light scattered by a random medium such as tissue is recorded as a function of scattering angle, enhanced backscattering manifests itself as a sharp peak centered around the backscattering direction. The scattered light intensity at the peak of an enhanced backscattering cone can be twice the incoherent background intensity outside of the enhanced backscattering cone. The intensity of enhanced backscattering quickly vanishes for angles away from the backward direction (Fig. 1). Our group has overcome these technological hurdles (the speckle and the narrow peak) by the discovery that under low spatially coherent illumination (i.e., spatial coherence length L_{cs} is much shorter than the transport mean free path for which light traveling in tissue is randomized, which is $\sim$1 mm in tissue; refs. 19–21). Thus, our low coherence innovation makes enhanced backscattering analysis of tissue feasible.

We used the alterations of LEBS spectra as a gauge of the microarchitectural consequences of the well-established genetic/epigenetic changes in the field effect. To quantitate these structural alterations, we used several previously validated optical variables. We have previously developed spectral slope as a marker of perturbations at the macromolecular complex to small organelle level (8, 25). As seen in Fig. 4, our studies in the azoxymethane-treated rat model show that LEBS spectral slope was decreased early during carcinogenesis, and this change progressed over time paralleling progression of carcinogenesis. Although the origin of microarchitectural alterations has yet to be identified, we speculate that the decrease in spectral slope may reflect aggregation of macromolecular complexes and other nanoscale intracellular structures, thus decreasing the number of smaller particles. We have to point out that the data acquired through LEBS are extraordinarily rich, and the algorithms that we have currently developed extract a minute portion of the total information. In cancer biology and clinical medicine, one commonly used tool for discerning structure in a complex data set is through principal component analysis. Thus, we also did principal component analysis of LEBS spectra. As shown above, this approach yielded highly significantly altered diagnostic markers in both the azoxymethane-treated rat and the MIN mouse. These variables were highly diagnostic at the earliest pre-ACF and adenoma phases and progressed over time in a manner consonant with neoplastic transformation.

We believe that one of the major reasons for the outstanding sensitivity of LEBS for early colon carcinogenesis is its depth selectivity. The ability to rigorously define the depth of tissue interrogated dramatically improves signal detection by excluding photons that have traveled deeper than the epithelium and also removing the distortion from submucosal hemoglobin. Furthermore, given that the biochemical and functional heterogeneity of colonocytes that is largely determined by the position in the crypt, the depth selectivity allows targeting of the region of the colonic crypt most likely to undergo carcinogenesis, thus enhancing the "signal-to-noise" ratio (29). Our data indicate that the most profound changes during early colon carcinogenesis occurred at $\sim$80 μm, which approximately corresponds to the base of the crypt (Fig. 3). Several lines of evidence suggest that the base of the crypt is the location for initiation of colon carcinogenesis (30). For instance, there is compelling evidence that adenomatous transformation (as evident by crypt branching) also starts at the base of the crypt (31). Furthermore, this is the region where the colonic stem cells reside. Emerging evidence suggest that stem cells can accumulate mutations over several decades and thus are initiating cells in colon carcinogenesis (22). In this regard, conditions with high risk of colorectal cancer, such as familial adenomatous polyposis, expansion of the stem cell population has been noted (32).

There are limitations/potential confounders to this work that need to be acknowledged. First, our data processing algorithms do not allow exploitation of the full potential of the data encoded by LEBS. Thus, it is conceivable that there may be LEBS markers that have a greater diagnostic accuracy. Another potential concern is the possibility that we are detecting early ACF or microadenomas. Although we can not completely exclude this possibility, the fact that >90% of tissue sites assessed by LEBS showed abnormalities at pre-ACF and preadenoma time points (e.g., 2 weeks after carcinogen administration in the azoxymethane-treated rat model and 6-week-old MIN mice) strongly argues against the hypothesis that the altered LEBS markers reflect detection of focal dysplasia. In the azoxymethane-treated rat, approximately one half of animals will develop tumors; thus, future studies will be necessary to show that enhanced backscattering markers not only identifies azoxymethane exposure but actually predicts the occurrence of biologically significant neoplasia. In this regard, our human data support the feasibility of developing these prediction rules. One could also argue that the 80-μm depth may not exactly correspond to the location of colonic stem cells. Clearly, our hypothesis that the optimal nature 80-μm depth is related to probing the stem cell compartment is conjecture because stem cells are notoriously difficult to identify. Given the need to do LEBS analysis on fresh, unfixed tissue, simultaneous measurement of LEBS signatures, putative stem cell marker (e.g., Musashi-1) is impossible (30). On the other hand, even if our biologically plausible explanation for the optimal nature of the 80-μm depth is incorrect, this does not alter the major thrust and clinical implications of our LEBS findings. Finally, our human data, whereas compelling, need to be considered pilot data that simply confirm the relevance of LEBS marker abnormalities to human colon carcinogenesis. Future studies will be needed to delineate the power of this novel approach to colorectal cancer screening.

In summary, we showed, for the first time, that a novel optics technology, LEBS spectroscopy was able to accurately risk stratify for colon carcinogenesis in two experimental models of colon carcinogenesis. These light scattering and thus nanoarchitectural/microarchitectural changes in colonic

epithelium preceded conventional biomarkers of colon carcinogenesis and progressed over time, mirroring the events in neoplastic transformation. Furthermore, preliminary human data support the clinical relevance. The long-term goal of this work will be to develop a means of risk-stratifying patients for colon carcinogenesis by means of LEBS assessment of easily accessible endoscopically normal mucosa (such as in the rectum) to identify patients harboring neoplastic lesions elsewhere in the colon and optimize decisions regarding an individual colorectal cancer screening modalities and intervals.

Acknowledgments

We thank Drs. Ewa Gliwa and Nahla Hasabou for their technical assistance.

References

1. Jemal A, Murray T, Ward E, et al. Cancer statistics 2005. CA Cancer J Clin 2005;55:10–30.
2. Winawer S, Fletcher R, Rex D, et al. Colorectal cancer screening and surveillance: clinical guidelines and rationale—update based on new evidence. Gastroenterology 2003;124:544–60.
3. Zack DL, Di Baise JK, Quigley EM, Roy HK. Colorectal cancer screening compliance by medicine residents: perceived and actual. Am J Gastroenterol 2001;96:3004–8.
4. Ahlquist DA, Skoletsky JE, Boynton KA, et al. Colorectal cancer screening by detection of altered human DNA in stool: feasibility of a multitarget assay panel. Gastroenterology 2000;119:1219–27.
5. Imperiale TF, Ransohoff DF, Itzkowitz SH, Turnbull BA, Ross ME. Colorectal Cancer Study Group. Fecal DNA versus fecal occult blood for colorectal-cancer screening in an average-risk population. N Engl J Med 2004;351:2704–14.
6. Fenlon HM, Nunes DP, Schroy PC, III, Barish MA, Clarke PD, Ferrucci JT. A comparison of virtual and conventional colonoscopy for the detection of colorectal polyps. N Engl J Med 1999;341:1496–503.
7. Cotton PB, Durkalski VL, Pineau BC, et al. Computed tomographic colonography (virtual colonoscopy): a multicenter comparison with standard colonoscopy for detection of colorectal neoplasia. JAMA 2004;291:1713–9.
8. Roy HK, Wali RK, Kim YL, Liu Y, Goldberg M, Backman V. Four-dimensional elastic light-scattering fingerprints as preneoplastic markers in the rat model of colon carcinogenesis. Gastroenterology 2004;126:1071–81.
9. Braakhuis BJ, Tabor MP, Kummer JA, Leemans CR, Brakenhoff RH. A genetic explanation of Slaughter's concept of field cancerization: evidence and clinical implications. Cancer Res 2003;63:1727–30.
10. Lewis JD, Ng K, Hung KE, et al. Detection of proximal adenomatous polyps with screening sigmoidoscopy: a systematic review and meta-analysis of screening colonoscopy. Arch Intern Med 2003;163:413–20.
11. Takayama T, Katsuki S, Takahashi Y, et al. Aberrant crypt foci of the colon as precursors of adenoma and cancer. N Engl J Med 1998;339:1277–84.
12. Lieberman DA, Weiss DG, Bond JH, Ahnen DJ, Garewal H, Chejfec G. Use of colonoscopy to screen asymptomatic adults for colorectal cancer. Veterans Affairs Cooperative Study Group 380. N Engl J Med 2000;343:162–8.
13. Schoenfeld P, Shad J, Ormseth E, et al. Military Colorectal Cancer Screening Trials Group. Predictive value of diminutive colonic adenoma trial: the PREDICT trial. Clin Gastroenterol Hepatol 2003;1:195–201.
14. Chen LC, Hao CY, Chiu YC, et al. Alteration of gene expression in normal-appearing colon mucosa of APCmin mice and human cancer patients. Cancer Res 2004;64:3694–700.
15. Cui H, Cruz-Correa M, Giardiello FM, et al. Loss of IGF2 imprinting: a potential marker of colorectal cancer risk. Science 2003;299:1753–5.
16. Backman V, Wallace MB, Perelman LT, et al. Detection of preinvasive cancer cells. Nature 2000;406:35–6.
17. Perelman LT, Backman V, Wallace, et al. Observation of periodic fine structure in reflectance from biological tissue: a new technique for measuring nuclear size distribution. Phys Rev Lett 1998;80:627–30.
18. Gurjar RS, Backman V, Perelman LT, et al. Imaging human epithelial properties with polarized light-scattering spectroscopy. Nat Med 2001;7:1245–8.
19. Kim YL, Liu Y, Turzhitsky VM, Roy HK, Wali RK, Backman V. Coherent backscattering spectroscopy. Opt Lett 2004;29:1906–8.
20. Kim YL, Liu Y, Wali RK, Roy HK, Backman V. Low-coherent backscattering spectroscopy for tissue characterization. Appl Opt 2005;44:366–77.
21. Kim YL, Liu Y, Turzhitsky VM, Wali RK, Roy HK, Backman V. Depth-resolved low-coherence enhanced backscattering. Opt Lett 2005;30:741–3.
22. Calabrese P, Tavare S, Shibata D. Pretumor progression: clonal evolution of human stem cell populations. Am J Pathol 2004;164:1337–46.
23. Wali RK, Roy HK, Kim YL, et al. Increased microvascular blood content is an early event in colon carcinogenesis. Gut 2005;54:654–60.
24. Born M, Wolf E. Principles of optics: electromagnetic theory of propagation, interference and diffraction of light. 7th ed. Cambridge (NY): Cambridge University Press; 1999. p. 572–80.
25. Roy HK, Kim YL, Wali RK, et al. Markers in preneoplastic intestinal mucosa: an accurate predictor of tumor risk in the MIN mouse. Cancer Epidemiol Biomarkers Prev 2005;14:1639–45.
26. Bernstein C, Bernstein H, Garewal H, et al. A bile acid-induced apoptosis assay for colon cancer risk and associated quality control studies. Cancer Res 1999;59:2353–7.
27. Anti M, Marra G, Armelao F, et al. Rectal epithelial cell proliferation patterns as predictors of adenomatous colorectal polyp recurrence. Gut 1993;34:525–30.
28. McGarrity TJ, Peiffer LP. Protein kinase C activity as a potential marker for colorectal neoplasia. Dig Dis Sci 1994;39:458–63.
29. Booth C, Brady G, Potten CS. Crowd control in the crypt. Nat Med 2002;8:1360–1.
30. Brittan M, Wright NA. Stem cell in gastrointestinal structure and neoplastic development. Gut 2004;53:899–910.
31. Preston SL, Wong WM, Chan AO, et al. Bottom-up histogenesis of colorectal adenomas: origin in the monocryptal adenoma and initial expansion by crypt fission. Cancer Res 2003;63:3819–25.
32. Kim KM, Calabrese P, Tavare S, Shibata D. Enhanced stem cell survival in familial adenomatous polyposis. Am J Pathol 2004;164:1369–77.